

Cyclometalated Gold(III) Complexes Containing N-Heterocyclic Carbene Ligands Engage Multiple Anti-Cancer Molecular Targets

Sin Ki Fung[†], Taotao Zou[†], Bei Cao, Pui-Yan Lee, Yi Man Eva Fung, Di Hu, Chun-Nam Lok, and Chi-Ming Che^{*}

Abstract: Metal N-heterocyclic carbene (NHC) complexes are a promising class of anti-cancer agents displaying potent *in vitro* and *in vivo* activities. Taking a multi-faceted approach employing two clickable photoaffinity probes, herein we report the identification of multiple molecular targets for anti-cancer active pincer gold(III) NHC complexes. These complexes display potent and selective cytotoxicity against cultured cancer cells and *in vivo* anti-tumor activities in mice bearing xenografts of human cervical and lung cancers. Our experiments revealed the specific engagement of the gold(III) complexes with multiple cellular targets, including HSP60, vimentin, nucleophosmin, and YB-1, accompanied by expected downstream mechanisms of action. Additionally, Pt^{II} and Pd^{II} analogues can also bind the cellular proteins targeted by the gold(III) complexes, uncovering a distinct pincer cyclometalated metal–NHC scaffold in the design of anti-cancer metal medicines with multiple molecular targets.

The success in treating certain cancers by cisplatin has stimulated tremendous efforts to develop next generation, metal-based anti-cancer drugs with improved efficacy but lower side effects.^[1] In this regard, other metal medicines besides cisplatin including carboplatin, oxaliplatin, satraplatin, NAMI-A, KP1019 and auranofin, have been reported to display potent anti-tumor activities, with some of them now in clinical trials or clinical use. In particular, gold complexes have been demonstrated to potentially overcome cisplatin resistance through their distinctly different anti-cancer mechanisms.^[2] However, the low physiological stability of both gold(I) and gold(III) complexes hampers their general therapeutic utility *in vivo*.^[3] By taking advantage of the strong σ -donor strength of N-heterocyclic carbene (NHC) ligand and the ease of ligand modification,^[4] we have reported a stable pincer-type cyclometalated gold(III) complex containing methyl-substituted NHC ligand, [Au^{III}(C[^]N[^]C)(NHC^{2Me})]OTf (**1a**, H₂C[^]N[^]C = 2,6-diphenylpyridine;

Figure 1) that is highly cytotoxic to cancer cells and is effective to inhibit tumor growth in a mouse model of human liver cancer.^[5] The pincer-type Pt^{II} and Pd^{II} complexes containing mono-anionic C[^]N[^]N (HC[^]N[^]N = 6-phenyl-2,2'-bipyridine) or N[^]C[^]N (N[^]CH[^]N = 1,3-di(pyridin-2-yl)benzene) ligands and ancillary NHC ligands, which are structural analogues of [Au^{III}(C[^]N[^]C)(NHC)]⁺ complexes, also display comparable cytotoxicity towards cancer cells and exhibit potent *in vivo* anti-tumor activities.^[6]

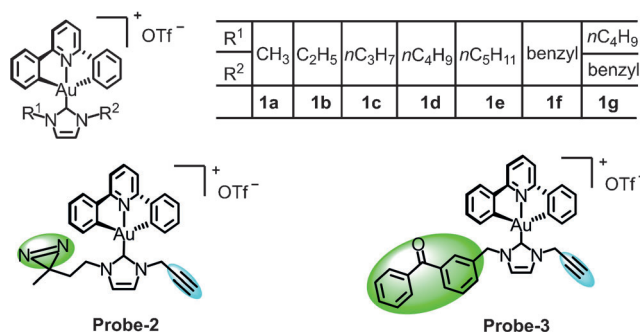


Figure 1. Chemical structure of gold(III) NHC complexes **1a–1g** and the chemical probes for target identification; green: photoaffinity unit; blue: clickable moiety.

Target identification utilizing photoaffinity groups together with clickable moieties recently emerged as a useful strategy to identify macromolecular binding partners for small organic molecules.^[7] Nevertheless, this approach has seldom been used for target identification of anti-cancer metal complexes,^[8] and only one example, combing benzophenone-based photoaffinity labelling and click chemistry for target identification of gold(III)porphyrin has been reported.^[8f] To circumvent the possible interference of the bulky benzophenone-containing functional groups to the interactions with bio-macromolecules,^[8f] herein, we introduced a small photoaffinity diazirine group and a clickable alkyne moiety on NHC to generate a chemical probe (probe-**2**) for target identification of [Au^{III}(C[^]N[^]C)(NHC)]OTf (Figure 1; the benzophenone analogue probe-**3** was prepared for comparison). By using these clickable photoaffinity probes, we found that a two-butyl substituted gold(III) NHC complex, which strongly inhibits tumor growth in multiple mouse models, is a multi-target, anti-cancer agent that can specifically bind six cellular proteins, all having been reported to be potential anti-cancer targets. The Pt^{II} and Pd^{II} analogues having the same structural geometry were also found to target these intracellular proteins.

[*] S. K. Fung,^[†] Dr. T. Zou,^[†] Dr. B. Cao, Dr. P.-Y. Lee, Dr. Y. M. E. Fung, Dr. D. Hu, Dr. C.-N. Lok, Prof. Dr. C.-M. Che
State Key Laboratory of Synthetic Chemistry, Institute of Molecular Functional Materials, Chemical Biology Centre and Department of Chemistry, The University of Hong Kong
Pokfulam Road, Hong Kong (China)
E-mail: cmche@hku.hk

Prof. Dr. C.-M. Che
HKU Shenzhen Institute of Research and Innovation
Shenzhen 518053 (China)

[†] These authors contributed equally to this work.

Supporting information for this article can be found under:
<http://dx.doi.org/10.1002/anie.201612583>.

We synthesized and examined the cytotoxicities of a series of gold(III) NHC complexes containing different substituents on their NHC ligands (Figure 1). As shown in Table S1, the increase of alkyl chain length on NHC resulted in enhanced cytotoxicity against HeLa (cervical), HCT116 (colon), and NCI-H460 (lung) cells; the IC_{50} gradually decreased from $2.04 \mu\text{M}$ (**1a**) to $0.36 \mu\text{M}$ (**1d**) for HeLa cells, with the same trend for HCT116 and NCI-H460 cells after a 72 h treatment. Probe-2 and probe-3 also showed potent cytotoxicity with IC_{50} being $0.23\text{--}0.68 \mu\text{M}$, indicating that the modification on NHC did not adversely affect the bioactivity. Importantly, all the gold(III) NHC complexes showed much higher cytotoxicity to HCT116 and NCI-H460 than to immortalized normal human hepatocyte (MIHA) cells. Complex **1d**, containing two *n*-butyl groups, displayed the highest selective cytotoxicity against cancer cells (> 30 -fold lower cytotoxicity against normal MIHA cells). We also tested the cytotoxicity of **1d** against 3D cancer cell spheroids which are more representative of malignant tumor tissues. While treatment of spheroids developed from HeLa cells with cisplatin at $100 \mu\text{M}$ caused only around 30% inhibition of spheroid growth after 72 h, **1d** treatment disintegrated the spheroids in a dose dependent manner and reduced the spheroid growth by about 70% at $40 \mu\text{M}$ (Figure S1 in the Supporting Information). Treatment of mice bearing xenografts of HeLa cancer with 3 mg kg^{-1} of **1d** inhibited tumor growth by 71% without affecting survival and significant influence on body weight (Figure 2a,b). Treatment of NCI-H460 xenografts with the same dosage of **1d** also resulted in a 53% tumor growth inhibition ($p < 0.05$) without negative effect on body weight (Figure S2).

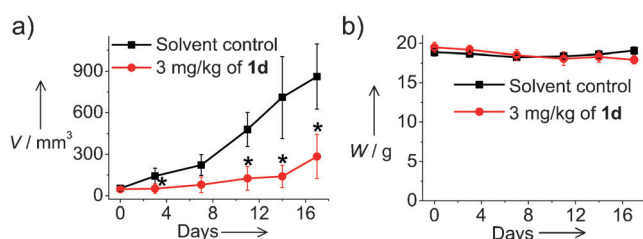


Figure 2. Anti-tumor activities of **1d**. a) Tumor volume (V) and b) body weight (W) of mice bearing HeLa xenografts after treatment with 3 mg kg^{-1} of **1d** ($n=3$) or solvent control ($n=4$). * $p < 0.05$.

We used probe-2, which contains a photo-activatable diazirine group that enables the gold(III) NHC complex to form covalent adducts with interacting proteins upon light irradiation and a clickable alkyne for linking to a reporter (e.g., fluorophore, biotin). HeLa cells were treated with probe-2 for 1 h and then irradiated at $\lambda = 365 \text{ nm}$ UV light, followed by a Cu^I -catalyzed click reaction with azido-biotin which was subsequently detected with a streptavidin-peroxidase conjugate (Figure 3a). As shown in Figure 3b, there are

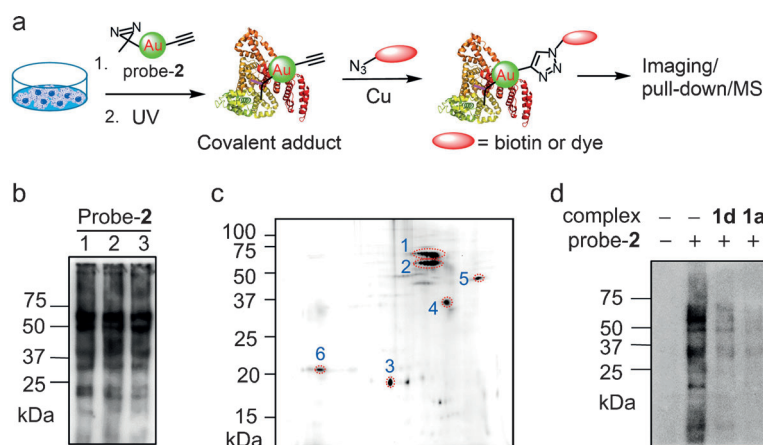


Figure 3. a) Schematic of procedure to identify cellular protein targets with probe-2. b) Detection of photoaffinity-labelled proteins in 1) HeLa, 2) NCI-H460, and 3) HCT116 cells treated with $5 \mu\text{M}$ probe-2. c) Fluorescence scanning of 2D gels of lysates from HeLa cells treated with probe-2, and clicked with azide-Cy5. MALDI-TOF indicates that each spot is HSP60 (1), vimentin (2), NDKA (3), nucleophosmin (4), YB-1 (5) and PRDX1 (6). d) Protein blotting of photoaffinity-labelled proteins in HeLa cells treated with $5 \mu\text{M}$ probe-2 for 1 h or $5 \mu\text{M}$ probe-2 + $10 \mu\text{M}$ of **1d** or **1a**, followed by irradiation and click reaction with biotin azide.

about six photoaffinity-labelled (biotinylated) proteins that were identified in the one-dimensional (1D) protein blot of the HeLa cell lysates. These bands were also observable in the protein samples from NCI-H460 and HCT116 cells treated with probe-2. When azido-Cy5 (a highly fluorescent cyanine dye) was used as the reporter (Figure 3c), six distinct fluorescent spots were detected in the two-dimensional (2D) gel electrophoresis of the cellular proteins from HeLa cells and identified to be mitochondrial heat shock protein 60 (HSP60), vimentin (VIM), nucleoside diphosphate kinase A (NDKA), nucleophosmin (NPM), nuclease-sensitive element binding protein (Y box binding protein, YB-1), and peroxiredoxin 1 (PRDX1) by tandem mass spectrometric analysis using MALDI-TOF mass spectrometry (Tables S2–S7). It is noteworthy that co-incubation of HeLa cells with probe-2 and two-fold of **1d** or **1a** significantly reduced the intensity of photoaffinity-labelled protein signals (Figure 3d). The proteins bound to probe-2 were also identified by HPLC-LTQ-Orbitrap MS analysis of the trypsin digests of the biotinylated proteins pulled down by streptavidin beads. Again, HSP60, vimentin, NDKA, nucleophosmin, and PRDX1 can be repeatedly identified as the proteins bound to probe-2 with high confidence (Table S8). Probe-3, which contains benzophenone instead of diazirine, displays lower photoaffinity towards cellular proteins compared to probe-2 (Figure S3a), but can still label four proteins, namely, vimentin, HSP60, nucleophosmin, and PRDX1 in HeLa cells (Figure S3b).

Cellular imaging experiments were carried out to examine the subcellular distribution of probe-2. HeLa cells were treated with probe-2, UV irradiation, and a click reaction with Alexa Fluor 488. As shown in the first column in Figure S4, probe-2 mainly localized to the cytoplasm with a small portion in the nucleus. This is consistent with the 2D gel results identifying vimentin, which is localized in the cytoplasm, as a major portion of the emissive spots, with the

nuclear nucleophosmin spot less emissive. We further investigated the co-localization of probe-2 with vimentin, HSP60, nucleophosmin and YB-1 by immunofluorescence. Figure S4 shows that all the protein immunofluorescence could be merged with the Alexa Fluor 488 fluorescence of probe-2 to a reasonable extent.

It should be emphasized that all six identified binding proteins have been described as potential anti-cancer targets.^[9] In the current study, we singled out HSP60, vimentin, nucleophosmin and YB-1 as proteins of interest and used the highly potent **1d** to test whether the binding interactions are associated with the anti-cancer activity. We first enriched probe-2 binding proteins using biotin affinity pull-down followed by western blotting and detection with specific antibodies. As shown in Figure 4a, the enriched probe-2 binding proteins can be detected by anti-HSP60, -vimentin, -nucleophosmin, and -YB-1 antibodies on the western blot. Importantly, **1d** at a 2-fold excess concentration can significantly attenuate the binding of probe-2 to HSP60, vimentin, nucleophosmin, and YB-1 (Figure 4a).

We subsequently examined whether the specific binding interactions could interfere the respective protein functions in cancer cells. HSP60 is a chaperone protein responsible for the transport of proteins into mitochondria and protein folding in the mitochondrial matrix.^[9d] We transfected a mitochondria-targeting green fluorescent protein (Mito-EGFP) that is known to be fluorescent only when it is properly folded by HSP60 in mitochondria.^[10] As presented in Figure 4b, while

the HeLa cells transfected with a GFP-expressing construct (EGFP) with no organelle-targeting property did not show obvious changes in fluorescence upon treatment with 0.5 or 1 μM of **1d**, the fluorescence intensity in HeLa cells transfected with Mito-EGFP was markedly reduced upon **1d** treatment in a dose dependent manner. In a typical HSP60 chaperone assay using denatured malate dehydrogenase (MDH) as the refolding substrate, HSP60 in combination with HSP10 can recover approximately 25 % of MDH activity, while HSP60/HSP10 in the presence of **1d** at 10 and 20 μM can only recover about 10 % and about 3 % of the MDH activity (Figure 4c). Although not to the same extent as **1d**, complex **1a**, probe-2 and probe-3 also strongly inhibited HSP60/HSP10 activity (Figure 4c).

Vimentin, an intermediate filament protein, is part of the cytoskeleton with a mesenchymal origin and a high expression in various cancers.^[9c] It has been demonstrated that direct interaction of anti-cancer agents (e.g., withaferin A) with vimentin can induce degradation of this protein and apoptotic cell death.^[11] HeLa cells were treated with increasing concentrations (0, 1, 3, and 5 μM) of **1d** for 24 h; western blot analysis revealed a dose-dependent decrease in full-length vimentin levels and an increase in the expression of a vimentin degradation product (Figure 4d). This degradation process is accompanied by gradually increased cleavage of poly (ADP-ribose) polymerase (PARP), caspase-9, and caspase-3 (Figure 4d), which suggests that apoptosis is triggered.

Nucleophosmin is a nucleolar protein involved in DNA replication and ribosome biogenesis.^[12] This protein is upregulated in cancer cells and can interact with p14^{ARF}, a positive regulator of tumor suppressor p53. As shown in Figure 4e, treatment of HeLa cells with 1–5 μM **1d** disrupted nucleophosmin oligomers (functional forms) in a dose-dependent manner, in association with a gradual formation of nucleophosmin monomers.^[9b] Meanwhile, an increased expression of both p53 protein levels and its Ser15 phosphorylation status was observed.

YB-1 is an oncogenic transcription factor that is overexpressed in many cancers.^[9a] Its expression is closely associated with drug resistance and YB-1 has been shown to control multidrug resistance 1 (*MDR1*) gene expression. Also, YB-1 is capable of promoting cell growth via transcriptional upregulation of epidermal growth factor receptor (EGFR). Knockdown of YB-1 expression by shRNA has been reported to inhibit tumor growth in vitro and in vivo.^[13] We found that treatment of HeLa cells with 1–5 μM of **1d** for 24 h significantly decreased YB-1 levels (Figure 4f). At the same time, the expression of EGFR was also significantly inhibited after treatment of HeLa cells with **1d** (Figure 4f), which is consistent with a previous observation that RNA silencing of YB-1 down-regulated EGFR expression.^[14]

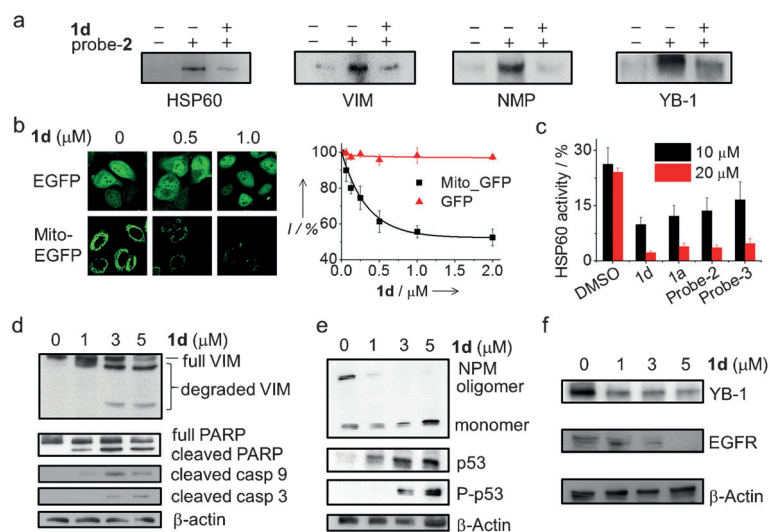


Figure 4. a) Western blot analysis of the cell lysates from cells labelled with or without probe-2 (5 μM) or with probe-2 (5 μM) in the presence of **1d** (10 μM) followed by click reaction with azido-biotin and pull-down with streptavidin beads. Nucleophosmin (NPM), vimentin (VIM), HSP60, or YB-1 antibodies were used for detection of the pull-down proteins. b) Inhibition of HSP60 activity in HeLa cells treated with **1d**. Left: representative fluorescence imaging of HeLa cells transfected with EGFP or Mito-EGFP followed by treatment with different concentrations of **1d**. Right: dose-dependent effects of **1d** on the EGFP and Mito-EGFP fluorescence intensities (I/I₀). c) Inhibition of chaperone activity of Hsp60 in MDH refolding. d)–f) Western blot analysis of HeLa cells treated with **1d** (0–5 μM) for 24 h. The cell lysates were resolved by polyacrylamide gel electrophoresis under denaturing conditions, except for nucleophosmin which was performed under native conditions, followed by western blot analysis of the indicated proteins.

Molecular docking and hybrid quantum mechanics/molecular mechanics (QM/MM) studies revealed that **1d** preferentially binds to the aromatic amino acid residues, including Tyr, Phe and Trp via π - π interactions with the $[\text{Au}(\text{C}^{\wedge}\text{N}^{\wedge}\text{C})]$ moiety (Figure S5a), in association with hydrophobic interactions (Figure S5b,c) with all the six binding proteins. Taken together, our data indicate that the direct binding interaction of **1d** with HSP60, vimentin, nucleophosmin, and YB-1 may result in the inhibition of HSP60 activity, degradation of vimentin, disruption of nucleophosmin oligomerization and downregulation of YB-1 in cancer cells, respectively. These processes either individually or synergistically lead to subsequent anti-cancer effects involving suppression of EGFR, induction of tumor suppressor p53 and activation of apoptotic caspases in cell death.

To obtain a holistic insight, proteomic analysis of the effects of **1d** on protein expression profiles in HeLa cells using HPLC-LTQ-Orbitrap MS was performed. A bioinformatics analysis of the proteomic data showed that the eukaryotic initiation factor 2 (eIF2) signaling pathway was predominantly modulated in HeLa cells treated with **1d** ($5\ \mu\text{M}$) for 6 h with high statistical significance (Table S9). eIF2 is an essential factor of the protein translation initiation complex in protein synthesis. The alpha subunit of eIF2 (eIF2 α) is subjected to inhibitory regulation by specific protein kinases via phosphorylation at Ser-51 under cellular stress.^[15] Three of the protein targets of **1d** identified by using probe-2, namely, vimentin, nucleophosmin, and YB-1, have been reported to directly or indirectly inhibit eIF2 α kinases, resulting in dephosphorylation of eIF2 α and the ensuing protein synthesis under normal conditions.^[16] Western blot analysis (Figure S6) showed that there was a significant time-dependent up-regulation of phosphorylated eIF2 α in the HeLa cells treated with **1d** ($5\ \mu\text{M}$), consistent with down-regulation of the eIF2 signaling pathway as revealed by the proteomic analysis. Thus the possibility exists that vimentin degradation, disruption of NMP oligomers and down-regulation of YB-1, all caused by **1d** treatment (Figure 4d-f), may result in inhibition (i.e. phosphorylation) of eIF2 α , leading to a global reduction in protein synthesis and hence anti-proliferative activities (Figure 5).^[15]

The analogue complexes $[\text{Pt}(\text{C}^{\wedge}\text{N}^{\wedge}\text{N})(\text{NHC})]^+$, $[\text{Pt}(\text{N}^{\wedge}\text{C}^{\wedge}\text{N})(\text{NHC})]^+$ and $[\text{Pd}(\text{C}^{\wedge}\text{N}^{\wedge}\text{N})(\text{NHC})]^+$ (**Pt-1a**, **Pt-1b**, **Pt-2a**, **Pt-2b**, **Pd-1**, Figure 6a) are highly stable, have the same cationic charge, share similar structural scaffold, and

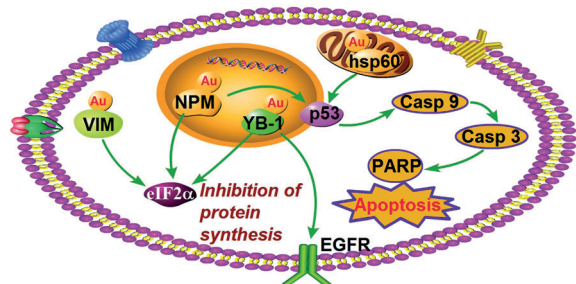


Figure 5. Proposed anti-cancer pathway induced by **1d**, according to proteomics data and western blot analyses.

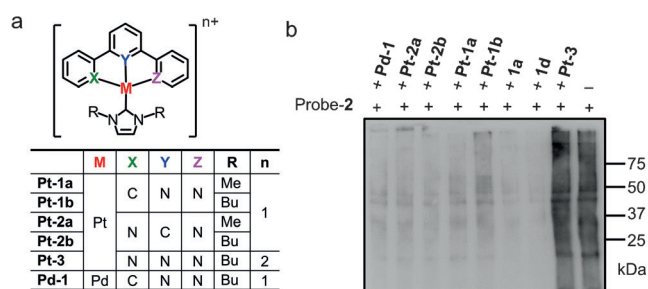


Figure 6. a) The chemical structure of Pt^{II} and Pd^{II} complexes.

b) Immunoblot analysis of photoaffinity-labelled proteins in HeLa cells treated with probe-2 and a twofold excess of a different Pt, Pd, or Au complex, followed by UV irradiation and click reaction with biotin azide.

displayed comparable cytotoxicities against cancer cells as the gold(III)-NHC analogues.^[6] In a competition experiment, co-incubating HeLa cells with probe-2 ($5\ \mu\text{M}$) and a 2-fold excess of any of the Pt or Pd complexes, **Pt-1a**, **Pt-1b**, **Pt-2a**, **Pt-2b**, or **Pd-1**, markedly decreased the band intensity as effectively as **1d** and **1a** (Figure 6b). However, **Pt-3**, which has one more positive charge, did not attenuate the band intensity. Taken together, the square planar mono-cationic Pt²⁺, Pd²⁺, and Au³⁺ complexes containing pincer type ligand and NHC ligand may share similar anti-cancer molecular targets in cancer cells.

In summary, the $[\text{Au}(\text{C}^{\wedge}\text{N}^{\wedge}\text{C})(\text{NHC})]^+$ complexes (as exemplified by **1d**) are a type of multi-target, anti-cancer agent, exhibiting potent in vitro and in vivo anti-cancer activities. We identified a number of intracellular proteins as the molecular targets of the gold(III) NHC complexes using clickable photoaffinity probes, and verified the ensuing anti-cancer effects. Interestingly, the Pt^{II} and Pd^{II} NHC analogues were found to compete with the gold(III) NHC complexes in binding these proteins, highlighting the structural importance of pincer-type metal complexes containing NHC ligands in their anti-cancer activities. Structural scaffolds targeting protein kinases using inert octahedral metal complexes have been developed by Meggers and co-workers.^[17] Since drug resistance is usually encountered for single-target anti-cancer agents as a result of naturally occurring genetic mutations,^[18] anti-cancer agents with multiple anti-cancer molecular targets could minimize drug resistance. For example, the FDA-approved Sorafenib and Sunitinib exhibit cumulative effects of targeting multiple tyrosine kinases and are superior to single-target drugs.^[19] The pincer-type gold(III), Pt^{II}, and Pd^{II} NHC complexes are promising candidate scaffolds to be developed as multi-target, anti-cancer agents with potentially low drug resistance.

Acknowledgements

This work was supported by the Innovation and Technology Fund (ITF-Tier 2 ITS/130/14FP), General Research Fund of Research Grants Council (HKU17300614), and a Special Equipment Grant of University Grants Committee (SEG_HKU02).

Conflict of interest

The authors declare no conflict of interest.

Keywords: anti-cancer mechanisms · gold · metal medicines · N-heterocyclic carbene · target identification

- [1] N. J. Farrer, P. J. Sadler in *Bioinorganic Medicinal Chemistry* (Ed.: E. Alessio), Wiley-VCH, Weinheim, **2011**, pp. 1–37.
- [2] a) P. J. Sadler, R. E. Sue, *Met.-Based Drugs* **1994**, *1*, 107–144; b) I. Ott, *Coord. Chem. Rev.* **2009**, *253*, 1670–1681; c) A. Bindoli, M. P. Rigobello, G. Scutari, C. Gabbiani, A. Casini, L. Messori, *Coord. Chem. Rev.* **2009**, *253*, 1692–1707; d) S. Nobili, E. Mini, I. Landini, C. Gabbiani, A. Casini, L. Messori, *Med. Res. Rev.* **2010**, *30*, 550–580; e) S. J. Berners-Price, A. Filipovska, *Metallomics* **2011**, *3*, 863–873; f) F. Cisnetti, A. Gautier, *Angew. Chem. Int. Ed.* **2013**, *52*, 11976–11978; *Angew. Chem.* **2013**, *125*, 12194–12196; g) T. Zou, C. T. Lum, C.-N. Lok, J.-J. Zhang, C.-M. Che, *Chem. Soc. Rev.* **2015**, *44*, 8786–8801; h) C. Nardon, D. Fregona, *Curr. Top. Med. Chem.* **2016**, *16*, 360–380.
- [3] a) A. Meyer, C. P. Bagowski, M. Kokoschka, M. Stefanopoulou, H. Alborzina, S. Can, D. H. Vlecken, W. S. Sheldrick, S. Wölfl, I. Ott, *Angew. Chem. Int. Ed.* **2012**, *51*, 8895–8899; *Angew. Chem.* **2012**, *124*, 9025–9030; b) T. Zou, C. T. Lum, S. S.-Y. Chui, C.-M. Che, *Angew. Chem. Int. Ed.* **2013**, *52*, 2930–2933; *Angew. Chem.* **2013**, *125*, 3002–3005; c) T. Zou, C. T. Lum, C.-N. Lok, W.-P. To, K.-H. Low, C.-M. Che, *Angew. Chem. Int. Ed.* **2014**, *53*, 5810–5814; *Angew. Chem.* **2014**, *126*, 5920–5924; d) C. Nardon, G. Boscutti, D. Fregona, *Anticancer Res.* **2014**, *34*, 487–492; e) C. Bazzicalupi, M. Ferraroni, F. Papi, L. Massai, B. Bertrand, L. Messori, P. Gratteri, A. Casini, *Angew. Chem. Int. Ed.* **2016**, *55*, 4256–4259; *Angew. Chem.* **2016**, *128*, 4328–4331.
- [4] a) D. A. Medvetz, K. M. Hindi, M. J. Panzner, A. J. Ditto, Y. H. Yun, W. J. Youngs, *Met.-Based Drugs* **2008**, 384010; b) H. G. Raubenheimer, S. Cronje, *Chem. Soc. Rev.* **2008**, *37*, 1998–2011; c) A. Gautier, F. Cisnetti, *Metallomics* **2012**, *4*, 23–32; d) C. Hu, X. Li, W. Wang, L. Deng, *Curr. Med. Chem.* **2014**, *21*, 1220–1230; e) M. Marinelli, C. Santini, M. Pellei, *Curr. Top. Med. Chem.* **2016**, *16*, 2995–3017; f) W. Liu, R. Gust, *Coord. Chem. Rev.* **2016**, *329*, 191–213.
- [5] J. J. Yan, A. L.-F. Chow, C.-H. Leung, R. W.-Y. Sun, D.-L. Ma, C.-M. Che, *Chem. Commun.* **2010**, *46*, 3893–3895.
- [6] a) R. W.-Y. Sun, A. L.-F. Chow, X.-H. Li, J. J. Yan, S. S.-Y. Chui, C.-M. Che, *Chem. Sci.* **2011**, *2*, 728–736; b) K. Li, T. Zou, Y. Chen, X. Guan, C.-M. Che, *Chem. Eur. J.* **2015**, *21*, 7441–7453; c) T. T. H. Fong, C. N. Lok, C. Y. S. Chung, Y. M. E. Fung, P. K. Chow, P. K. Wan, C. M. Che, *Angew. Chem. Int. Ed.* **2016**, *55*, 11935–11939; *Angew. Chem.* **2016**, *128*, 12114–12118.
- [7] a) K. T. Barglow, B. F. Cravatt, *Nat. Methods* **2007**, *4*, 822–827; b) B. J. Leslie, P. J. Hergenrother, *Chem. Soc. Rev.* **2008**, *37*, 1347–1360; c) J. Park, S. Oh, S. B. Park, *Angew. Chem. Int. Ed.* **2012**, *51*, 5447–5451; *Angew. Chem.* **2012**, *124*, 5543–5547; d) Y. Su, J. Ge, B. Zhu, Y.-G. Zheng, Q. Zhu, S. Q. Yao, *Curr. Opin. Chem. Biol.* **2013**, *17*, 768–775; e) S. Ziegler, V. Pries, C. Hedberg, H. Waldmann, *Angew. Chem. Int. Ed.* **2013**, *52*, 2744–2792; *Angew. Chem.* **2013**, *125*, 2808–2859; f) M. Koh, J. Park, J. Y. Koo, D. Lim, M. Y. Cha, A. Jo, J. H. Choi, S. B. Park, *Angew. Chem. Int. Ed.* **2014**, *53*, 5102–5106; *Angew. Chem.* **2014**, *126*, 5202–5206; g) J. Ge, C.-W. Zhang, X. W. Ng, B. Peng, S. Pan, S. Du, D. Wang, L. Li, K.-L. Lim, T. Wohland, S. Q. Yao, *Angew. Chem. Int. Ed.* **2016**, *55*, 4933–4937; *Angew. Chem.* **2016**, *128*, 5017–5021.
- [8] a) C. X. Zhang, P. V. Chang, S. J. Lippard, *J. Am. Chem. Soc.* **2004**, *126*, 6536–6537; b) G. Zhu, S. J. Lippard, *Biochemistry* **2009**, *48*, 4916–4925; c) J. D. White, M. F. Osborn, A. D. Moghaddam, L. E. Guzman, M. M. Haley, V. J. DeRose, J. Am. Chem. Soc. **2013**, *135*, 11680–11683; d) S. Ding, X. Qiao, J. Suryadi, G. S. Marrs, G. L. Kucera, U. Bierbach, *Angew. Chem. Int. Ed.* **2013**, *52*, 3350–3354; *Angew. Chem.* **2013**, *125*, 3434–3438; e) M. V. Babak, S. M. Meier, K. V. M. Huber, J. Reynisson, A. A. Legin, M. A. Jakupec, A. Roller, A. Stukalov, M. Gridling, K. L. Bennett, J. Colinge, W. Berger, P. J. Dyson, G. Superti-Furga, B. K. Keppler, C. G. Hartinger, *Chem. Sci.* **2015**, *6*, 2449–2456; f) D. Hu, Y. Liu, Y.-T. Lai, K.-C. Tong, Y.-M. Fung, C.-N. Lok, C.-M. Che, *Angew. Chem. Int. Ed.* **2016**, *55*, 1387–1391; *Angew. Chem.* **2016**, *128*, 1409–1413.
- [9] a) M. Kuwano, Y. Oda, H. Izumi, S.-J. Yang, T. Uchiumi, Y. Iwamoto, M. Toi, T. Fujii, H. Yamana, H. Kinoshita, T. Kamura, M. Tsuneyoshi, K. Yasumoto, K. Kohno, *Mol. Cancer Ther.* **2004**, *3*, 1485–1492; b) Y. Jian, Z. Gao, J. Sun, Q. Shen, F. Feng, Y. Jing, C. Yang, *Oncogene* **2009**, *28*, 4201–4211; c) A. Satelli, S. Li, *Cell. Mol. Life Sci.* **2011**, *68*, 3033–3046; d) A. Pace, G. Barone, A. Lauria, A. Martorana, P. A. Palumbo Piccionello, P. Pierro, A. Terenzi, A. M. Almerico, S. Buscemi, C. Campanella, F. Angileri, F. Carini, G. Zummo, E. Conway de Macario, F. Cappello, A. J. L. Macario, *Curr. Pharm. Des.* **2013**, *19*, 2757–2764; e) Y.-F. Wang, C.-J. Chang, J.-H. Chiu, C.-P. Lin, W.-Y. Li, S.-Y. Chang, P.-Y. Chu, S.-K. Tai, Y.-J. Chen, *Oncotarget* **2014**, *5*, 7392–7405; f) C. Ding, X. Fan, G. Wu, *J. Cell. Mol. Med.* **2016**, DOI: 10.1111/jcmm.12955.
- [10] T. J. Corydon, J. Hansen, P. Bross, T. G. Jensen, *Mol. Genet. Metab.* **2005**, *85*, 260–270.
- [11] P. Bargagna-Mohan, A. Hamza, Y.-e. Kim, Y. Khuan Ho, N. Mor-Vaknin, N. Wendschlag, J. Liu, R. M. Evans, D. M. Markovitz, C.-G. Zhan, K. B. Kim, R. Mohan, *Chem. Biol.* **2007**, *14*, 623–634.
- [12] a) M. J. Lim, X. W. Wang, *Cancer Detect. Prev.* **2006**, *30*, 481–490; b) H. J. Chan, J. J. Weng, B. Y. M. Yung, *Biochem. Biophys. Res. Commun.* **2005**, *333*, 396–403; c) J. K. Box, N. Paquet, M. N. Adams, D. Boucher, E. Bolderson, K. J. O'Byrne, D. J. Richard, *BMC Mol. Biol.* **2016**, *17*, 19.
- [13] H. Wang, R. Sun, M. Gu, S. Li, B. Zhang, Z. Chi, L. Hao, *PLoS One* **2015**, *10*, e0127224.
- [14] C. Lee, J. Dhillon, M. Y. C. Wang, Y. Gao, K. Hu, E. Park, A. Astanehe, M.-C. Hung, P. Eirew, C. J. Eaves, S. E. Dunn, *Cancer Res.* **2008**, *68*, 8661–8666.
- [15] T. Chen, D. Ozel, Y. Qiao, F. Harbinski, L. Chen, S. Denoyelle, X. He, N. Zvereva, J. G. Supko, M. Chorev, J. A. Halperin, B. H. Aktas, *Nat. Chem. Biol.* **2011**, *7*, 610–616.
- [16] a) Q. Pang, T. A. Christianson, T. Koretsky, H. Carlson, L. David, W. Keeble, G. R. Faulkner, A. Speckhart, G. C. Bagby, *J. Biol. Chem.* **2003**, *278*, 41709–41717; b) K. A. Wehner, S. Schütz, P. Sarnow, *Mol. Cell. Biol.* **2010**, *30*, 2006–2016; c) S. Chatterjee, A. C. Panda, S. K. Berwal, R. K. Sreejith, C. Ritvika, V. Seshadri, J. K. Pal, *FEBS Lett.* **2013**, *587*, 474–480.
- [17] E. Meggers, *Angew. Chem. Int. Ed.* **2011**, *50*, 2442–2448; *Angew. Chem.* **2011**, *123*, 2490–2497.
- [18] C. Holohan, S. Van Schaeybroeck, D. B. Longley, P. G. Johnston, *Nat. Rev. Cancer* **2013**, *13*, 714–726.
- [19] a) S. Giordano, A. Petrelli, *Curr. Med. Chem.* **2008**, *15*, 422–432; b) J.-J. Lu, W. Pan, Y.-J. Hu, Y.-T. Wang, *PLoS One* **2012**, *7*, e40262.

Manuscript received: December 28, 2016







Final Article published: ■ ■ ■ ■ ■ ■ ■ ■ ■ ■

Communications

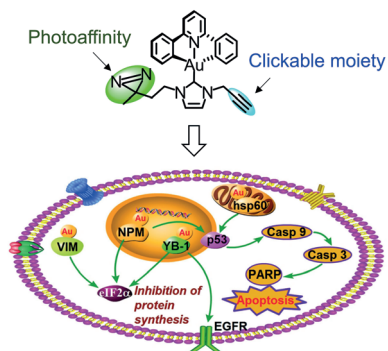
VIP

Gold Anti-Cancer Agents



S. K. Fung, T. Zou, B. Cao, P.-Y. Lee,
Y. M. E. Fung, D. Hu, C.-N. Lok,
C.-M. Che*      

Cyclometalated Gold(III) Complexes
Containing N-Heterocyclic Carbene
Ligands Engage Multiple Anti-Cancer
Molecular Targets



On target: Anti-cancer active pincer cyclometalated gold(III) complexes containing N-heterocyclic carbene ligands have been identified to be a type of multi-target, anti-cancer agent by using a combined photoaffinity labelling and click chemistry approach. The Pd^{II} and Pt^{II} analogues can competitively bind to the same cellular targets.